

Directed Coulomb Explosion regime of ion acceleration from mass limited targets by linearly and circularly polarized laser pulses.

S. S. Bulanov,^{1,2} D. W. Litzenberg,³ K. Krushelnick,¹ and A. Maksimchuk¹

¹*FOCUS Center and Center for Ultrafast Optical Science,
University of Michigan, Ann Arbor, Michigan 48109, USA*

²*Institute of Theoretical and Experimental Physics, Moscow 117218, Russia*

³*Department of Radiation Oncology, University of Michigan, Ann Arbor, Michigan 48109, USA*

We consider the Directed Coulomb Explosion regime of ion acceleration from ultra-thin double layer (high Z/low Z) mass limited targets. In this regime the laser pulse evacuated the electrons from the irradiated spot and accelerates the remaining ion core in the direction of the laser pulse propagation. Then the moving ion core explodes due to the excess of positive charge forming a moving charge separation field that accelerates protons from the second layer. The utilization of the mass limited targets increases the effectiveness of the acceleration. It is also shown that different parameters of laser-target configuration should be chosen to ensure optimal acceleration by either linearly polarized or circularly polarized pulses.

PACS numbers: 52.38.Kd, 29.25.Ni, 52.65.Rr, 41.85.Ct

Keywords: Ion acceleration, laser-plasma interaction, Coulomb Explosion

I. INTRODUCTION

The acceleration of ion beams in the intense laser pulse interaction with gaseous and solid density targets is one of the most promising applications of future laser systems [1]. These beams can be used in hadron therapy [2], fusion ignition [3], proton radiography [4], and for injection into conventional accelerators [5]. The possibility of effective ion acceleration was proved in a number of experiments, which showed the maximum ion energy up to tens of MeV. This process also was extensively studied analytically and in particle-in-cell (PIC) computer simulations, which showed the possibility of ion acceleration up to the energy of several hundred of MeV or even to the several GeV depending on the parameters of laser-plasma interaction [6, 7].

There are a number of ion acceleration regimes discussed in the literature: (i) Target Normal Sheath Acceleration (TNSA) [8]; (ii) Coulomb Explosion (CE) [9]; (iii) Radiation Pressure (RPDA) [10]; and (iv) acceleration from near critical density targets (NCD) [11]. The TNSA regime is the first identified with regard to ion acceleration from thin foils. It comes into play when the laser pulse is not intense enough to penetrate the target and instead it launches hot electrons from the front of the target that go through the target and establish a sheath field at its back. This field accelerates the ions. When the pulse is intense enough to evacuate all the electrons from the focal spot the Coulomb Explosion of the bare ion core follows. And when the pulse is able to push the foil as a whole this is the Radiation pressure regime of ion acceleration. The TNSA, CE and RPDA regimes use thin foils of solid density as targets, in contrast to that the NCD regime utilizes targets of near critical density. The ion acceleration in this case is due to the longitudinal electric field established at the back of the target by the exiting the propagation channel magnetic field, which in its turn is generated by electrons accelerated in the wake of the laser pulse. Recently several mechanisms of ion acceleration were reported in the literature: the TNSA coupled to the energy conversion from an expanding electron cloud to the expanding ion cloud under the action of burning through the foil laser pulse [12], the CE optimized by injecting a proton bunch into the longitudinal field [13], and the Directed Coulomb Explosion (DCE), which is the effective combination of the RPDA and CE regimes [14]. Also the dependence of ion acceleration on different parameters of interaction were reported in Refs. [15].

In this paper we study the DCE regime of ion acceleration in the intense laser pulse interaction with ultra-thin double layer (high Z/low Z) [2, 16, 17] mass limited targets. The DCE regime comes into play when the laser pulse is able not only to evacuate the electrons from the irradiated spot, but also to accelerate the remaining ion core by the radiation pressure. In this case the ion core experiences Coulomb Explosion while being set in motion. This means that the ion core transforms into an ion cloud expanding predominantly in the laser pulse propagation direction. There is a charge separation field moving in front of the positively charged ion cloud. In this field the protons of the second layer are accelerated. In the present paper we study the effect of mass limited targets on the proton acceleration because in this case the influence of the electron return current, that can compensate the positive charge in the irradiated spot, is reduced. Also the evacuation of the electrons and the acceleration of the ion core are more effective. We also consider the effects of different laser pulse polarizations. We compare the acceleration by the linearly polarized pulses with the acceleration by circularly polarized ones. We optimize the acceleration process in both cases varying the thickness and radius of the target.

The paper is organized as follows. In section 2 we review the properties of the DCE regime of ion acceleration. The results of 2D PIC simulations are presented in section 3. We conclude in section 4.

II. THE DIRECTED COULOMB EXPLOSION REGIME OF ION ACCELERATION.

In this section we review the DCE regime of ion acceleration from ultra-thin double-layer (high Z /low Z) foils of solid density described in Ref. [14]. The principal scheme of the laser-foil interaction is shown in Fig. 1. In contrast to the TNSA or CE or any other mentioned above scheme of ion acceleration the DCE regime comes into play as an effective combination of radiation pressure and coulomb explosion. It happens when the laser pulse is able not only to expel the electron from the focal spot but also to accelerate the remaining ion core by the radiation pressure. Then the moving ions experience Coulomb explosion and the protons from the second layer are accelerated by the moving charge separation electric field. The proton energy can be estimated in three steps as was shown in Ref. [14]. First, the velocity of the foil that is due to the radiation pressure should be calculated. Then the energy gain due to the Coulomb Explosion in the moving with the foil velocity reference frame should be obtained. The final estimate is made by transforming back to the laboratory frame.

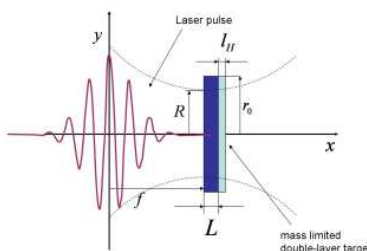


FIG. 1: (color on-line) The principal scheme of laser pulse interaction with a mass limited double-layer solid density ultra-thin target.

Let us estimate the proton energy gain in DCE regime of proton acceleration from double-layer target in the nonrelativistic case. The radiation pressure is proportional to the intensity of the pulse, $I \sim E_L^2$, where $E_L = E_L(t - x(t)/c)$ is the laser pulse electric field. The total momentum gain due to the radiation pressure is $P \sim E_L^2 \tau \sim W/R^2$, here τ is the duration of the laser pulse, W is the laser pulse energy and R is the radius of the focal spot. If we normalize the total momentum of the accelerated fraction of the foil on the number of ions in this fraction we obtain for the momentum of accelerated ions $p_i/m_i c = W/N_i m_i c^2$, where $N_i = \pi R^2 L n_i$ is the number of ions in the accelerated fraction. Here n_i is the ion density of the foil.

In the moving reference frame ($V/c = p_i/m_i c$) the protons will acquire the energy $\mathcal{E}' = mv^2/2$ due to the longitudinal charge separation electric field produced by the heavy ion core. \mathcal{E}' , can be estimated as the energy gain by a charged particle accelerated near the surface of a charged disk and the acceleration distance is of the order of the disk radius, r_0 :

$$\mathcal{E}' = 2\pi^2 m_e c^2 \frac{n_e}{n_{cr}} \frac{L r_0}{\lambda^2}. \quad (1)$$

Here $n_{cr} = \omega^2 m_e / 4\pi e^2$ is the critical plasma density, ω is the laser frequency.

The velocity in the laboratory frame is $V_{lab} = v + V$ and energy of the accelerated protons reads as follows

$$\mathcal{E} = \mathcal{E}' + \frac{p_i}{m_i c} \sqrt{2\mathcal{E}' m_p c^2}. \quad (2)$$

As it was shown in Ref. [14], for a 500 TW laser pulse interacting with a 0.1λ thick, $n_e = 400n_{cr}$ aluminum foil with a layer of hydrogen on the back this formula gives a 100% energy increase over the value acquired in the static charge separation field. A more detailed analysis of the acceleration process was carried out in Ref. [14] based on the results of Ref. [10] for the RPDA regime. In Ref. [14] the solution of the equation of the foil motion under the action of the radiation pressure is given, and the energy gain of protons due to DCE is obtained in general case. In the nonrelativistic case the formula (5) of Ref. [14] reduces to Eq. (2) of the present paper.

We should mention here that in order to expel all the electrons and achieve the coulomb explosion the following condition on laser electromagnetic vector potential $a = 0.85[I(W/cm^2)\lambda^2(\mu m)10^{-18}]^{1/2}$ and foil thickness L must be

satisfied [14]:

$$a = \pi \frac{n_e L}{n_{cr} \lambda}. \quad (3)$$

From this condition one can see that for circularly and linearly polarized pulses of the same total EM energy different foil thicknesses follow. It is due to the fact that the value of vector potential for linearly polarized pulse is square root of two times bigger than that of the circularly polarized one. Though this will lead to the reduction of the proton energy gain due to the coulomb explosion (see Eq.(2)), it will also lead to the increase of foil velocity due to radiation pressure (see Eq.(1)). The estimates carried out based on Eq.(4) show a 10-20% difference between the maximum energy of protons accelerated in either circularly or linearly polarized pulse interaction with foils of different thicknesses. In order to obtain this estimate we also varied the radius of the irradiated spot.

The utilization of the mass limited targets leads to different effects on the effectiveness of proton acceleration in the DCE regime. First of all, such targets provide a way to have a clean DCE regime without the influence of the return current. Also the smaller is the radius of the target the more monoenergetic the protons become. However the reduction of the target size leads to the reduction of the charge separation field and thus to the reduction of \mathcal{E}' . For the mass limited target with the radius smaller than the focal spot radius, R , we will have the following estimate

$$\mathcal{E}_{r_0 > R} = \mathcal{E}'(R/r_0) + (p_i/m_i c) \sqrt{2\mathcal{E}' m_p c^2} \sqrt{R/r_0}. \quad (4)$$

We see that the maximum proton energy increases with the increase of the target radius and reaches the value obtained in Eq. (4) for $r_0 = R$. However when the radius of the of the target exceeds the focal spot radius the effects of charge compensation by the return current come into play effectively reducing the estimate of the maximum proton energy made in Eq. (4). That is why the mass limited target with the radius of about the focal spot radius should maximize the accelerated proton energy. In the next section we will test this estimate against the results of 2D PIC simulations.

III. 2D PIC SIMULATION RESULTS

Here we report on the results of the 2D PIC simulations of an intense laser pulse interaction with a double layer mass limited target. We use the 2D PIC code REMP (relativistic electromagnetic particle), which is a mesh code based on particle-in-cell method [18]. The grid mesh size is $\lambda/200$, space and time scales are given in units of λ and $2\pi/\omega$, respectively, the simulation box size is $20\lambda \times 10\lambda$. The 500 TW (peak intensity of 3×10^{22} W/cm²) 30 fs duration laser pulse, introduced at the left boundary and propagating along the x axis from left to right, is tightly focused ($f/D = 1.5$, spot size is 1λ full width at half maximum, FWHM) at the foil, which is placed at the distance of $f = 3.33\lambda$ from the left boundary. The pulse is either linearly (along the z axis) or circularly polarized. The target is composed of two layers: high Z, fully ionized silicon Si^{+14} with an electron density of $600n_{cr}$, thickness L ; and low Z layer, ionized hydrogen (H^+ , $n_H = 30n_{cr}$), with a thickness l_H . As mentioned above, the material of the foil is assumed to be fully ionized. This is justified since the intensity needed to fully ionize silicon is approximately 10^{21} W/cm², while we use in simulations the intensity at least one order of magnitude larger. So the foil will become fully ionized well before the arrival of the pulse peak and can be modeled as a double layer slab of the overdense plasma.

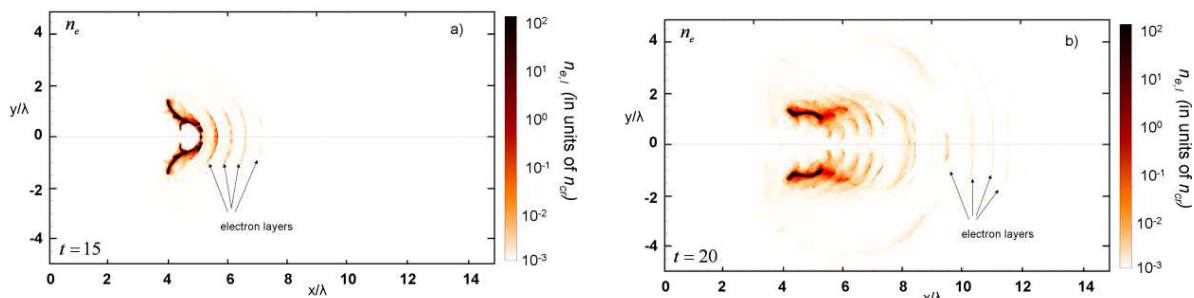


FIG. 2: (color on-line) The distributions of electron density at $t = 15$ (a) and $t = 20$ (b) for a 500 TW linearly polarized laser pulse interaction with a double layer (Si+H) mass limited target, $R = 1.5\lambda$.

In order to illustrate the interaction of a laser pulse with mass limited target we present Fig. 2 where the distribution of electron density for two time instants is shown. One can see that under the action of intense laser pulse the electrons

that are not in the focal spot are pushed aside, and those that are in the focal spot are evacuated in the form of thin layers, as was pointed out in Ref. [19]. These layers, flying with the velocity approaching the speed of light, can be utilized as relativistic mirrors to create ultra-short electromagnetic pulses from the counterpropagating pulses as was shown in Ref. [20]. This is an illustration that relativistic mirrors can be created not only in the laser interaction with gaseous targets but also in the interaction with solid density targets, in the regime that is considered in regard with the ion acceleration. The formation of these layers can clearly be seen in the electron distribution in phase space (see Fig. 3).

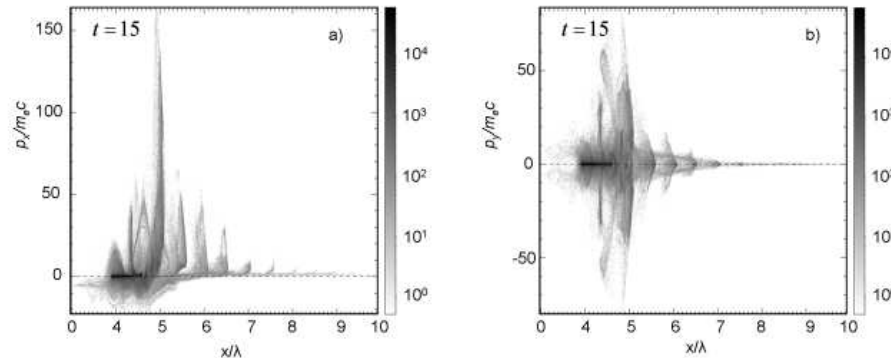


FIG. 3: The distribution of electrons in phase space (x, p_x) (a) and (x, p_y) (b) at $t = 15$ for a 500 TW linearly polarized laser pulse interaction with a double layer (Si+H) mass limited target, $R = 1.5\lambda$.

At the time when the electrons are pushed from the focal spot, the heavy ions of the first layer begin to move under the action of the radiation pressure, see Fig. 4a. While in motion the heavy ion layer experience Coulomb explosion due to the excess of positive charge. It leads to the transformation of the heavy ion layer into the expanding predominantly in the direction of laser pulse propagation ion cloud, see Fig. 4b. This expanding cloud generates a charge separation longitudinal electric field (Fig. 5), which accelerates the protons of the second layer.

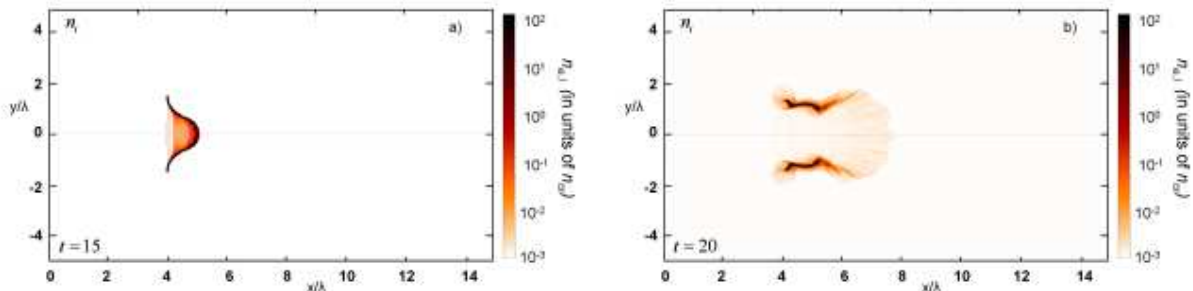


FIG. 4: (color on-line) The distribution ion density at $t = 15$ (a) and $t = 20$ (b) for a 500 TW linearly polarized laser pulse interaction with a double layer (Si+H) mass limited target, $R = 1.5\lambda$.

The protons first experience the acceleration due to the radiation pressure and then the longitudinal charge separation field comes into play. The protons are accelerated in a form of a thin layer flying in front of the expanding heavy ion cloud almost in all directions (Fig. 6). However the most energetic protons, as can be seen from the proton distribution in (p_x, p_y) plane (Fig. 7a), are going in the laser propagation direction.

In order to compare the cases of linear and circular polarizations we show the distribution of protons in (p_x, p_y) plane in both cases. It can be easily seen that the maximum energy of protons is almost the same, as well as the angular distribution. The larger thickness of the proton distribution in the case of circular polarization should lead to a broader peak in proton spectrum.

The spectra of accelerated protons in the cases of circular and linear polarization of the laser pulse are shown in Fig. 8. These protons are contained inside an angle of 5° from the target normal. Here a 500 TW tightly focused ($f/D=1$) laser pulse interacted with a 0.1λ thick disk with the radius of 1.5λ for linear and 1.0λ for circular polarization. Both spectra have maxima around $\mathcal{E} = 320$ MeV and extend to the maximum energy of $\mathcal{E} = 370$ MeV. However the protons accelerated by the linearly polarized pulse demonstrate a monoenergetic behavior with a sharp peak in spectrum with

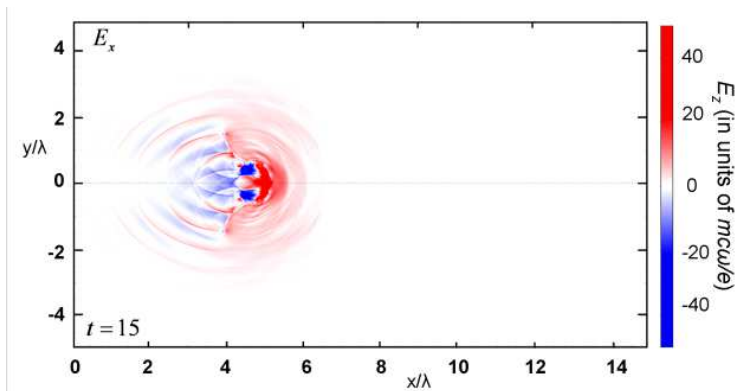


FIG. 5: (color on-line) The distribution of the x-component of electric field at $t =$ for a 500 TW linearly polarized laser pulse interaction with a double layer (Si+H) mass limited target, $R = 1.5\lambda$.

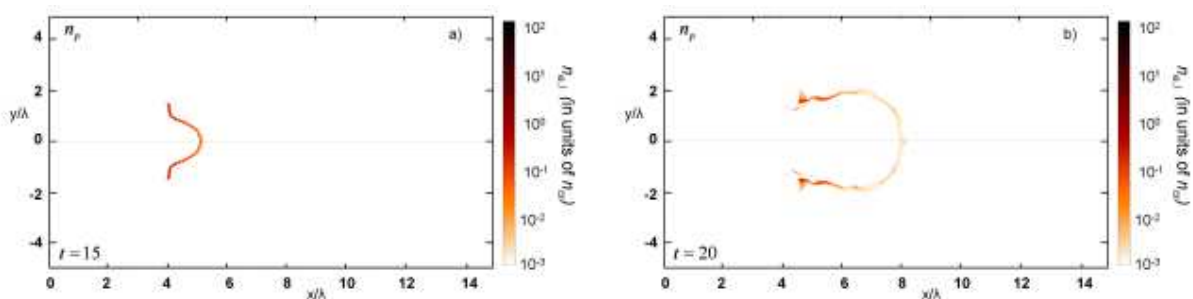


FIG. 6: (color on-line) The distribution proton density at $t = 15$ (a) and $t = 20$ (b) for a 500 TW linearly polarized laser pulse interaction with a double layer (Si+H) mass limited target, $R = 1.5\lambda$.

$\Delta\mathcal{E}/\mathcal{E} \sim 1\%$. Whereas in the case of circular polarization of the laser pulse the protons have a wide distribution with $\Delta\mathcal{E}/\mathcal{E} \sim 25\%$. This could be expected from the analysis of the proton distribution in (p_x, p_y) plane.

As it was mentioned above the proton maximum energy depends on the size of a mass limited target. In Fig. 9 we present several dependencies of maximum proton energy on the radius of the target for different target thicknesses and different laser polarizations.

However all these curves has one feature in common. At first, the maximum proton energy steadily increases with the increase of the transverse size of the target. They have a maximum around $R = \lambda$, *i.e.* when the target is about the size of the focal spot. Further increase of the target size affects the maximum proton energy only slightly. This result can be expected from the analytical estimate, carried out in the previous section.

We should also note that the absolute maxima of \mathcal{E}_{max} for circular and linear polarizations are very close. However they clearly correspond to different target thicknesses. As it was mentioned in the previous section is due to the fact that for circular polarization the optimal target thickness is smaller then for linear one since a in the case of circular polarization is smaller.

IV. CONCLUSION.

In this paper we studied the Directed Coulomb Explosion regime of ion acceleration from double-layer solid density mass limited targets. As it was shown in Refs. [14] this regime which is an effective combination of the radiation pressure and coulomb explosion mechanisms of ion acceleration allows for the production of quasimonoenergetic protons beams which are highly sought for a number of applications. In this regime the laser pulse not only removes the electrons from the irradiated area but also accelerates the remaining ion core. Thus this core is transformed into an expanding predominantly in the direction of the laser pulse propagation ion cloud. This positively charged cloud is the source of the longitudinal electric field that accelerated the light ions from the second layer.

Here we focused on the study of DCE regime of acceleration in laser pulse interaction with mass limited targets. Such targets allow for the reduction of the electron return current that can compensate the positive charge in the

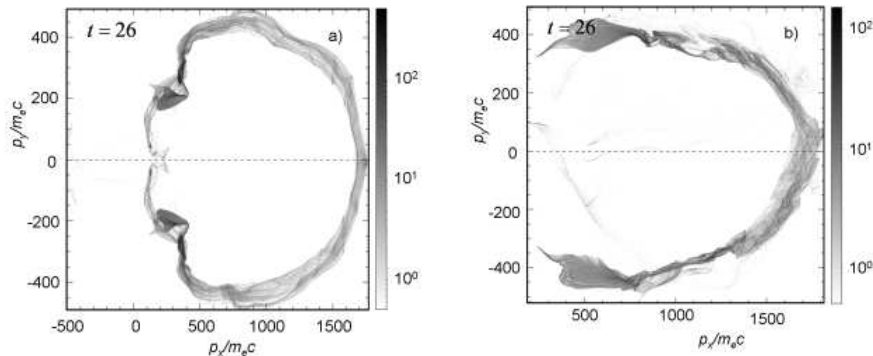


FIG. 7: The distribution of protons in (p_x, p_y) plane accelerated by linearly (a) and circularly (b) polarized laser pulses.

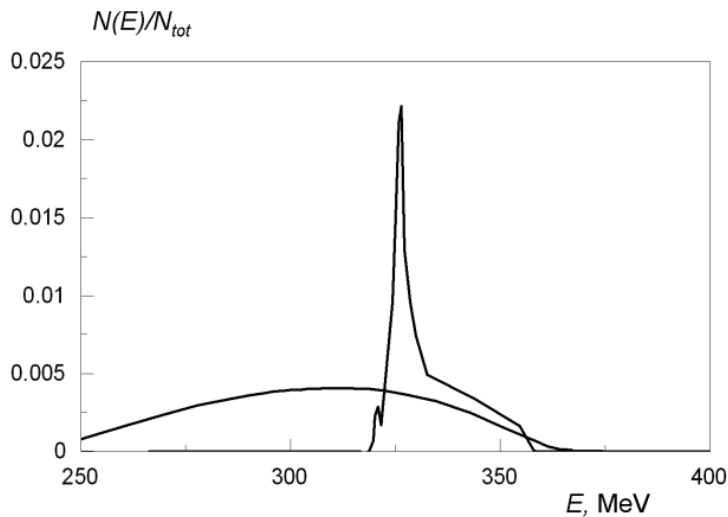


FIG. 8: The spectra of protons accelerated inside an angle of 5° to the target normal at $t = 26$ for 500 TW linearly and circularly polarized laser pulses interacting with a double layer (Si+H) mass limited target, $R = 1.5\lambda$ for linear polarization and $R = 1\lambda$ for circular polarization.

irradiated spot. Also the use of mass limited target increases the effectiveness of electron expulsion from the focal spot and the monoenergeticity of accelerated protons. We studied the dependency of the proton maximum energy on the transverse size of the target. As it increases so does the maximum energy of protons due to the fact that the energy gain in Coulomb field increases while the energy gain due to radiation pressure stays the same. When the radius of the target reaches the same size as the focal spot radius this increase stops. Further increase of the target transverse size leads to the slow reduction of the maximum proton energy in most cases which can be attributed to the effect of the return current. That is why we argue that the mass limited targets with the transverse size matching the focal spot of the laser pulse are most favorable for the proton acceleration in the DCE regime. However this statement is true for the targets having optimal thicknesses.

We were also interested in the effect of laser pulse polarization on the maximum proton energy due to the fact that recently a number of papers appeared claiming the advantages of using the laser pulses with circular polarization for ion acceleration. We indeed find that the optimum conditions for ion acceleration differ for circular and linear polarizations. It is however connected with the fact that for circular polarization the maximum achievable value of the electric field is smaller than that for linear polarization. That is why the optimal target thickness should be smaller in the former case. We should note here that smaller target thickness does not necessarily lead to the reduction of the maximum proton energy because of the reduction of the coulomb repulsion field of the bare ion core. As the energy gain due to the Coulomb Explosion decreases, the energy gain due to the Radiation Pressure increases. That is why we did not find a strong difference between the maximum proton energies obtained in either circularly or linearly polarized pulse interactions with solid density foils in the DCE regime of ion acceleration for a wide range

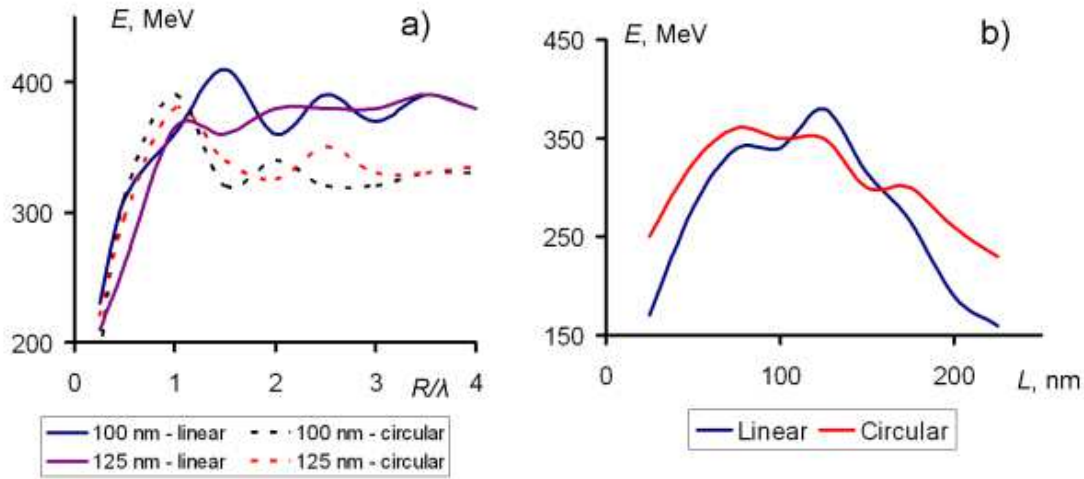


FIG. 9: The dependencies of the proton maximum energy (a) on target radius for different target thicknesses and (b) on target thickness for different laser polarizations for a 500 TW laser pulse interaction with a double layer (Al+H) mass limited target

of parameters.

Acknowledgments

This work was supported by the National Science Foundation through the Frontiers in Optical and Coherent Ultrafast Science Center at the University of Michigan. The authors would like to thank Dr. T. Zh. Esirkepov for providing REMP code for simulations. The authors acknowledge fruitful discussions with Prof. V. Yu. Bychenkov.

-
- [1] A. Maksimchuk, S. Gu, K. Flippo, D. Umstadter, and V. Y. Bychenkov, *Phys. Rev. Lett.* **84**, 4108 (2000); E. L. Clark, K. Krushelnick, J. R. Davies, M. Zepf, M. Tatarakis, F. N. Beg, A. Machacek, P. A. Norreys, M. I. K. Santala, I. Watts, and A. E. Dangor, *Phys. Rev. Lett.* **84**, 690 (2000); R. A. Snavely, *et al.*, *Phys. Rev. Lett.* **85**, 2945 (2000).
- [2] S. V. Bulanov and V. S. Khoroshkov, *Plasma Phys. Rep.* **28**, 453 (2002); E. Fourkal, B. Shanine, M. Ding, J. S. Li, T. Tajima, C.-M. Ma, *et al.*, *Med. Phys.* **29**, 2788 (2002).
- [3] M. Roth, T. E. Cowan, M. H. Key, S. P. Hatchett, C. Brown, W. Fountain, J. Johnson, D. M. Pennington, R. A. Snavely, S. C. Wilks, K. Yasuike, H. Ruhl, F. Pegoraro, S. V. Bulanov, E. M. Campbell, M. D. Perry, and H. Powell, *Phys. Rev. Lett.* **86**, 436 (2001); V. Yu. Bychenkov, W. Rozmus, A. Maksimchuk, D. Umstadter and C. E. Capjack, *Plasma Phys. Rep.* **27**, 1017 (2001); A. Macchi, A. Antonicci, S. Atzeni, D. Batani, F. Califano, F. Cornolti, J. J. Honrubia, T. V. Lisseikina, F. Pegoraro, and M. Temporal, *Nucl. Fusion* **43**, 362 (2003); J. J. Honrubia, J. C. Fernandez, M. Temporal, B. M. Hegelich, and J. Meyer-ter-Vehn, *Physics of Plasmas* **16**, 102701 (2009).
- [4] M. Borghesi, J. Fuchs, S. V. Bulanov, A. J. Mackinnon, P. K. Patel, and M. Roth, *Fusion Science and Technology* **49**, 412 (2006).
- [5] K. Krushelnick, E. L. Clark, R. Allott, F. N. Beg, C. N. Danson, A. Machacek, V. Malka, Z. Najmudin, D. Neely, P. A. Norreys, M. R. Salvati, M. I. K. Santala, M. Tatarakis, I. Watts, M. Zepf, A. E. Dangor, *Plasma Science, IEEE Transactions on* **28**, 1184 - 1189 (2000).
- [6] T. Zh. Esirkepov, *et al.*, *JETP Lett.* **70**, 82 (1999); A. M. Pukhov, *Phys. Rev. Lett.* **86**, 3562 (2001); Y. Sentoku, *et al.*, *Appl. Phys. B* **74**, 207 (2002); A. J. Mackinnon, Y. Sentoku, P. K. Patel, D. W. Price, S. Hatchett, M. H. Key, C. Andersen, R. Snavely, and R. R. Freeman, *Phys. Rev. Lett.* **88**, 215006 (2002).
- [7] S. V. Bulanov, *et al.*, *JETP Lett.* **71**, 407 (2000); Y. Sentoku, *et al.*, *Phys. Rev. E* **62**, 7271 (2000); H. Ruhl, S. V. Bulanov, T. E. Cowan, T. V. Liseikina, P. Nickles, F. Pegoraro, M. Roth, W. Sandner, *Plasma Phys. Rep.* **27**, 411 (2001).
- [8] S. C. Wilks, A. B. Langdon, T. E. Cowan, M. Roth, M. Singh, S. Hatchett, M. H. Key, D. Pennington, A. MacKinnon, and R. A. Snavely, *et al.*, *Phys. Plasmas* **8**, 542 (2001).

- [9] S. V. Bulanov, T. Zh. Esirkepov, V. S. Khoroshkov, A. V. Kuznetsov and F. Pegoraro, Phys. Lett. A **299**, 240 (2002); E. Fourkal, I. Velchev, and C.-M. Ma, Phys. Rev. E **71**, 036421 (2005).
- [10] T. Esirkepov, M. Borghesi, S. V. Bulanov, G. Mourou, and T. Tajima, *et al.*, Phys. Rev. Lett. **92**, 175003 (2004).
- [11] A. V. Kuznetsov, T. Zh. Esirkepov, F. F. Kamenets, and S. V. Bulanov, Fiz. Plazmy **27**, 225 (2001) [Plasma Phys. Rep. **27**, 211 (2001)]; Y. Sentoku, T. V. Liseikina, T. Zh. Esirkepov, F. Califano, N. M. Naumova, Y. Ueshima, V. A. Vshivkov, Y. Kato, K. Mima, K. Nishihara, F. Pegoraro, and S. V. Bulanov, Phys. Rev. E **62**, 7271 - 7281 (2000); K. Matsukado, T. Esirkepov, K. Kinoshita, H. Daido, T. Utsumi, Z. Li, A. Fukumi, Y. Hayashi, S. Orimo, M. Nishiuchi, S. V. Bulanov, T. Tajima, A. Noda, Y. Iwashita, T. Shirai, T. Takeuchi, S. Nakamura, A. Yamazaki, M. Ikegami, T. Mihara, A. Morita, M. Uesaka, K. Yoshii, T. Watanabe, T. Hosokai, A. Zhidkov, A. Ogata, Y. Wada, and T. Kubota, Phys. Rev. Lett. **91**, 215001 (2003); S. S. Bulanov, V. Yu. Bychenkov, V. Chvykov, G. Kalinchenko, D. W. Litzenberg, T. Matsuoka, A. G. R. Thomas, L. Willingale, V. Yanovsky, K. Krushelnick, and A. Maksimchuk, Phys. Plasmas **17**, 1 (2010).
- [12] L. Yin, B. J. Albright, B. M. Hegelich, K. J. Bowers, K. A. Flippo, T. J. T. Kwan, and J. C. Fernandez, Phys. Plasmas **14**, 056706 (2007).
- [13] I. Velchev, E. Fourkal, and C.-M. Ma, Phys. Plasmas **14**, 033106 (2007).
- [14] S. S. Bulanov, A. Brantov, V. Yu. Bychenkov, V. Chvykov, G. Kalinchenko, T. Matsuoka, P. Rousseau, S. Reed, V. Yanovsky, D. W. Litzenberg, and A. Maksimchuk, Med. Phys. **35**, 1770 (2008); S. S. Bulanov, A. Brantov, V. Yu. Bychenkov, V. Chvykov, G. Kalinchenko, T. Matsuoka, P. Rousseau, V. Yanovsky, D. W. Litzenberg, K. Krushelnick, and A. Maksimchuk, Phys. Rev. E **78**, 026412 (2008).
- [15] J. Davis and G. M. Petrov, Phys. Plasmas **16**, 023105 (2009); G. M. Petrov and J. Davis, Appl. Phys. B **96**, 773 (2009); J. Davis and G. M. Petrov, Phys. Plasmas **16**, 044503 (2009).
- [16] T. Zh. Esirkepov *et al.*, Phys. Rev. Lett. **89**, 175003 (2002).
- [17] H. Schwoerer, S. Pfoth, O. Jackel, K. U. Amthor, B. Liesfeld, W. Ziegler, R. Sauerbrey, K. W. Ledingham, and T. Esirkepov, Nature **439**, 445 (2006).
- [18] T. Zh. Esirkepov, Comput. Phys. Comm. **135**, 144 (2001).
- [19] K. I. Popov, V. Yu. Bychenkov, W. Rozmus, S. S. Bulanov, and R. D. Sydora, Phys. Plasmas **16**, 053106 (2009).
- [20] S. S. Bulanov, A. Maksimchuk, K. Krushelnick, K. I. Popov, V. Yu. Bychenkov, and W. Rozmus, Phys. Lett. A **374**, 476–480 (2010).